Atmospheric
Chemistry
and Physics

Supplement of

The effectiveness of the coagulation sink of 3–10 nm atmospheric particles

Runlong Cai et al.

Correspondence to: Runlong Cai (runlong.cai@helsinki.fi)

Theoretical coagulation coefficient

The coagulation coefficient accounting for the van der Waals force was theoretically predicted using the hard-sphere coefficient and a multiplicative collision enhance factor, i.e.,

$$\beta = \beta^{\mathrm{HS}} \cdot E \tag{S1}$$

where β is the coagulation coefficient (cm^3 s^{-1}) with contributions from the van der Waals force, β^{HS} is the hard-sphere coagulation coefficient (cm^3 s^{-1}), and E is the enhancement factor (-).

For particles in the continuum regime with a very small Knudsen number (Kn) of particles, β^{HS} can be expressed as

$$\beta_{\mathrm{C}}^{\mathrm{HS}} = 2\pi(d_1 + d_1)(D_1 + D_2) \tag{S2}$$

where the subscript C is short for continuum, d_1 and d_2 are the sizes (nm) of colliding particles, and D is particle diffusivity (m^2 s^{-1}).

For particles in the free molecular regime with a very large Knudsen number (-) of particles, β^{HS} can be expressed as

$$\beta_{\mathrm{FM}}^{\mathrm{HS}} = \frac{\pi}{4}(d_1 + d_1)^2 \sqrt{c_1^2 + c_2^2} \tag{S3}$$

where the subscript FM is short for free molecular and c is the thermal velocity (m s^{-1}) of particles.

The value of β^{HS} in the transition regime can be computed using the formula in Lehtinen and Kulmala (2003),

$$\beta^{\mathrm{HS}} = 2\pi(d_1 + d_1)(D_1 + D_2) \frac{1 + \mathrm{Kn}}{1 + 0.377\mathrm{Kn} + \frac{4}{3\alpha}\mathrm{Kn}(1 + \mathrm{Kn})} \tag{S4}$$

$$\mathrm{Kn} = \frac{2\lambda}{d_1 + d_2} \tag{S5}$$

$$\lambda = \frac{3(D_1 + D_2)}{\sqrt{c_1^2 + c_2^2}} \tag{S6}$$

where α is the mass accommodation coefficient characterizing the effectiveness of coagulation (-) and λ is the mean free path (m) of particles. It can be demonstrated that Eq. S4 converges to Eqs. S2 and S3 at the continuum limit (Kn $\rightarrow$ 0) and the free molecular limit (Kn $\rightarrow \infty$), respectively.

The van der Waals enhancement factor was computed using the formulae reported in Chan and Mozurkewich (2001), which were fitted to the numerical solution to the integral from Sceats (1989). For particles in the continuum regime,

$$E(0) = 1 + 0.0757\ln(1 + A') + 0.0015[\ln(1 + A')]^3 \tag{S7}$$

$$A' = \frac{A}{kT}\frac{4d_1 d_2}{(d_1 + d_2)^2} \tag{S8}$$

where A is the Hamaker constant (J), k is the Boltzmann constant (J K^{-1}) and T is temperature (K).

For particles in the free molecular regime, the enhancement factor can be calculated using

$$E(\infty) = 1 + \frac{\sqrt{A'/3}}{1 + 0.0151\sqrt{A'}} - 0.186\ln(1 + A') - 0.0163[\ln(1 + A')]^3. \tag{S9}$$

For particles in the transition regime, we computed the enhancement factor using an interpolation formula given in (Alam, 1987),

$$E = \frac{E(0)}{1 + \frac{E(0)}{E(\infty)} \cdot x}(1 + x) \tag{S10}$$

$$x = \frac{8(D_1 + D_2)}{(d_1 + d_2)\sqrt{c_1^2 + c_2^2}} \tag{S11}$$

We also computed the enhance factor using alternative interpolation formulae reported in Sceats (1989) and Ouyang et al. (2012). According to Sceats (1989),

$$E = \frac{\beta(A/kT)}{\beta(0)} \tag{S12}$$

$$\beta(A/kT) = \beta_{FM}^{HS} \cdot E(A/kT, \infty) \cdot \left(\sqrt{1 + t_{12}(A/kT)^2} - t_{12}(A/kT)\right) \tag{S13}$$

$$t_{12}(A/kT) = \frac{\beta_{FM}^{HS} \cdot E(A/kT, \infty)}{2\beta_c^{HS} \cdot E(A/kT, 0)} \tag{S14}$$

where $\beta(0)$ can be calculated using Eq. S13 with $A = 0$.

According to Ouyang et al. (2012),

$$E = \frac{H(A/kT, Kn')}{H(0, Kn')} \tag{S15}$$

$$H(A/kT, Kn') = \frac{4\pi Kn'^2 + 25.836Kn'^3 + \sqrt{8\pi} \cdot 11.211Kn'^4}{1 + 3.502Kn' + 7.211Kn'^2 + 11.211Kn'^3} \tag{S16}$$

$$Kn'(A/kT) = \frac{2\sqrt{kTm_{12}}}{f_{12}(d_1 + d_2)}\frac{E(0)}{E(\infty)} \tag{S17}$$

where m_{12} is the reduced mass of particles and f_{12} is the reduced friction factor.

Figure S1 shows the theoretical enhancement factor for the collision between a particle with size d_p and a 100 nm particle. The Hamaker constant was assumed to be 8.9×10^{-20} J. As shown in Fig. S1, the value of E approaches $E(0)$ and $E(\infty)$ as Kn approaches 0 and ∞, respectively. For the collision between a 3-10 nm particle and a 100 nm particle, Kn ranges from 1.0 to 1.9. Correspondingly, the value of E computed using Eqs. 10 ranges from 1.4 to 1.5. Eqs. 10, 12, and 15 are consistent with each other with a difference smaller than 4 % for the test particles in this study, though it is noted in Ouyang et al. (2012) that there may be uncertainties in Eq. S15 for in the presence of van der Waals enhancement.
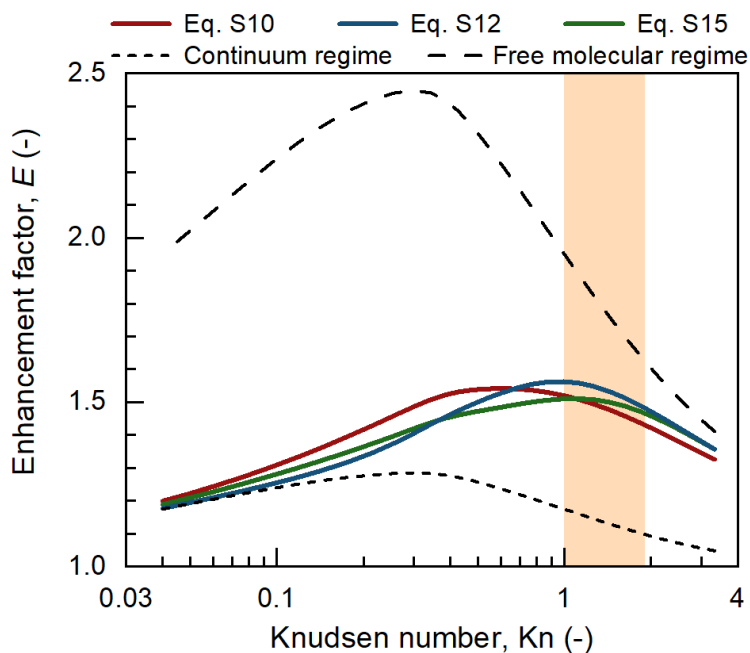
Figure S1. The van der Waals enhancement factor for the collision between a 1-1000 nm particle and a 100 nm particle. The Hamaker constant was assumed to be 8.9×10^{-20} J and particle density was assumed to be 2160 kg m^{-3}. The dashed lines indicate the enhancement factor calculated using the formulae for the continuum regime (Eq. S7) and the free molecular regime (Eq. S9). The shaded area indicates the Knudsen number of particles used in the chamber experiments.
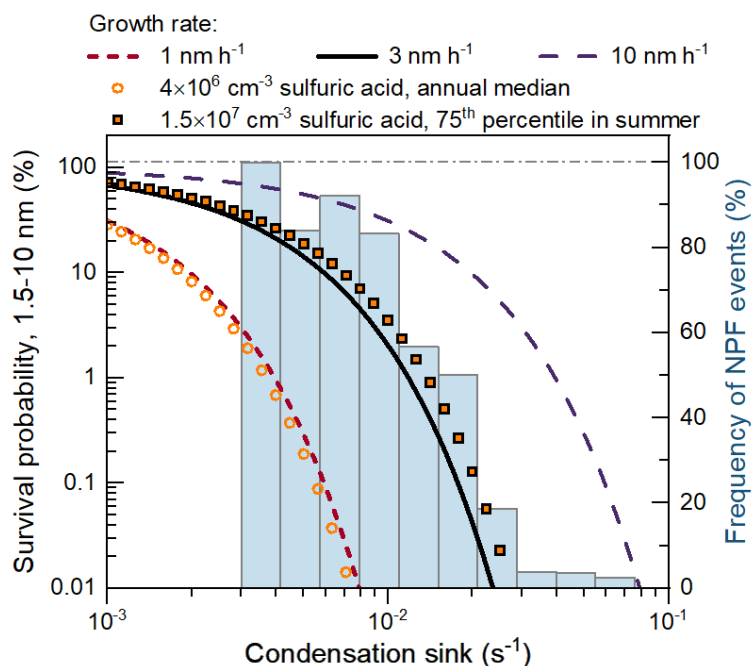

Figure S2. The theoretical survival probability of 1.5-10 nm new particles versus the measured frequency of new particle formation events in urban Beijing as a function of the condensation sink. The particle survival probability is

calculated assuming an effective coagulation sink. The condensation sink characterizes the size-dependent coagulation sink during each new particle formation event. The NPF frequency is determined as the ratio of NPF days to all the measurement days within the given condensation sink range. The lower limits of the vertical survival probability axis in this figure and Figure 7 in the main text are determined according to the measured median survival probability of new particles and particle formation rate in urban Beijing.
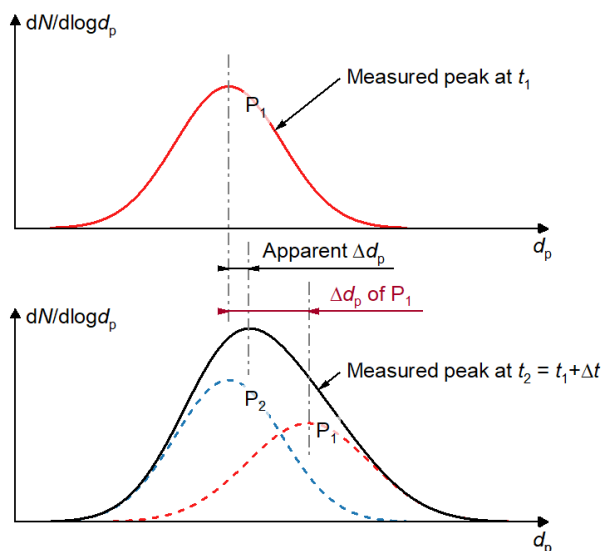

Figure S3. Schematic diagram for illustrating the underestimation of particle grow rate (GR) retrieved using the mode-fitting method. The mode-fitting method tracks the increase in a representative particle diameter (d_p) of a growing aerosol population (e.g., P_1) as a function of time (t). The representative d_p is usually the peak diameter of aerosol number size distribution ($dN/dlogd_p$). For instance, the peak diameter of aerosol population P_1 grows by Δd_p after Δt, and GR can be estimated using $\Delta d_p/\Delta t$. This estimated GR can be further corrected to disentangle the influences of coagulation.

However, a particle source, e.g., nucleation, may cause a significant underestimation in the retrieved GR. As shown in this figure, assuming a new aerosol population P_2 is formed during Δt. The measured aerosol size distribution at t_2 is the sum of the distributions of P_1 and P_2. As a result, the apparent Δd_p calculated using the measured distributions is smaller than the Δd_p of P_1, causing an underestimated GR. A more complicated scenario with continuous particle formation and growth is given in Figure S4, which also shows an underestimation of the mode-fitting method due to the influence of particle source.
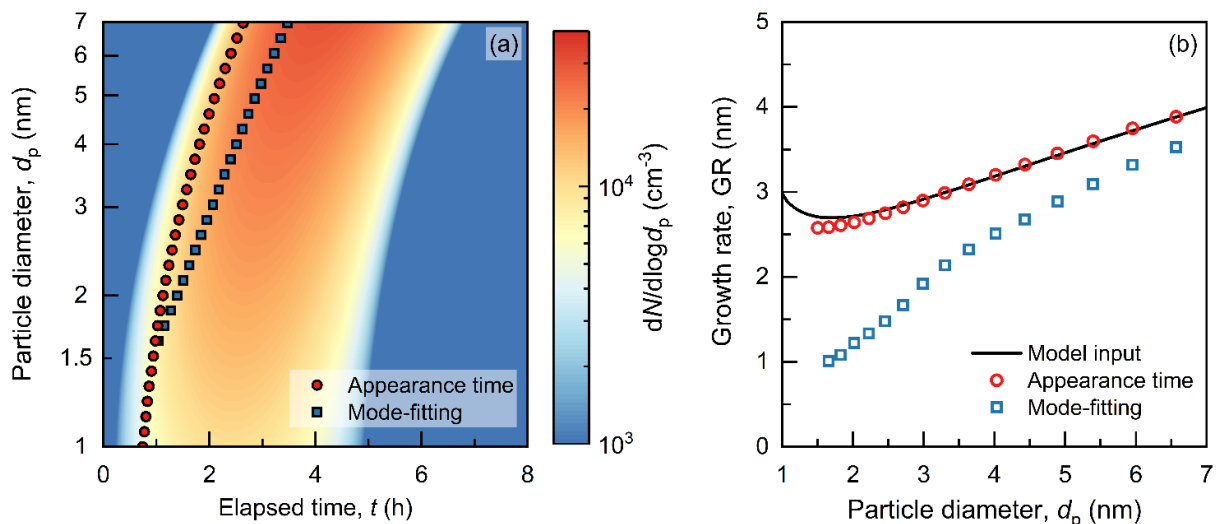
Figure S4. (a) Simulated particle size distribution ($dN/d\log d_p$) and diameter-time (d_p-t) relationship used for growth rate (GR) calculation. (b) Growth rates retrieved using the appearance time method and the mode-fitting method. The evolution of particle size distribution is simulated using a discrete aerosol model (Li and Cai, 2020). The input nucleation rate is time-dependent and the input particle growth rate (GR_{input}) is time-and-size dependent. The influences of coagulation on the GR retrieved using the appearance time method (GR_{app}) are corrected. The GR_{input} shown in panel (b) is calculated following the d_p-t relationship of the appearance time method. Due to the time-dependence of GR_{input}, the GR_{input} following d_p-t relationship of the mode-fitting method (not shown) is higher than that for the appearance time method, yet the difference is minor (5 % on average) for this simulation.

As shown in panel (b), GR_{app} is consistent with GR_{input}, indicating good accuracy of the appearance method for this simulation. The GR retrieved using the mode-fitting method (GR_{mode}) is significantly underestimated because of the influence of nucleation. This underestimation increases as the particle size decreases towards the critical cluster size, at which new particles are added to the simulation system.

Table S1. Parameters for the coagulation experiments.

Composition	d_p (nm)[*]	Kn (-)[**]	N_{sub10} (cm^{-3})[***]	β_{meas} (cm^3 s^{-1})	E_{meas} (-)
NaCl	3.6	1.72	11.0	1.89×10^{-7}	1.55
	3.7	1.70	10.6	1.74×10^{-7}	1.49
	4.0	1.63	55.2	1.76×10^{-7}	1.71
	5.0	1.45	210.5	1.22×10^{-7}	1.66
	10.0	0.99	895.3	4.25×10^{-8}	1.68
NH$_4$HSO$_4$	5.0	1.31	10.5	1.25×10^{-7}	1.59
	7.0	1.10	34.8	8.07×10^{-8}	1.73
	10.0	0.90	266.4	4.88×10^{-8}	1.81
Organics	6.6	1.00	77.5	1.05×10^{-7}	1.90
	9.5	0.82	155.5	4.47×10^{-8}	1.42
	12.4	0.71	414.9	3.58×10^{-8}	1.71

Meas is short for measurement.

[*]: d_p is the size of small particles. The size of large particles is 100 nm.

[**]: computed using Eq. S5

[***]: For NaCl and NH$_4$HSO$_4$ particles, N_{sub10} is the concentration of small particles in the chamber when the 100-nm particle concentration was 0 in Fig. 3. For organic particles, N_{sub10} is the concentration of small particles in the chamber for $t = 0$ in Fig. 5, and it is the mean value of repeated experiments. The concentration of 100 nm particles can be found in the horizontal axis of Fig. 3 and the legend of Fig. 5.

Reference

Alam, M. K.: The Effect of van der Waals and Viscous Forces on Aerosol Coagulation, Aerosol Science and Technology, 6, 41-52, 10.1080/02786828708959118, 1987.

Lehtinen, K. E., and Kulmala, M.: A model for particle formation and growth in the atmosphere with molecular resolution in size, Atmospheric Chemistry and Physics, 3, 251–257, 10.5194/acp-3-251-2003, 2003.

Li, C., and Cai, R.: Tutorial: The discrete-sectional method to simulate an evolving aerosol, Journal of Aerosol Science, 150, 105615, 10.1016/j.jaerosci.2020.105615, 2020.

Ouyang, H., Gopalakrishnan, R., and Hogan, C. J., Jr.: Nanoparticle collisions in the gas phase in the presence of singular contact potentials, J Chem Phys, 137, 064316, 10.1063/1.4742064, 2012.

Sceats, M. G.: Brownian coagulation in aerosols—the role of long range forces, Journal of Colloid and Interface Science, 129, 105-112, 10.1016/0021-9797(89)90419-0, 1989.